NUCLEAR DATA AND MEASUREMENTS SERIES

ANL/NDM-61

Fast-Neutron Total and Scattering Cross Sections of ^{58}Ni

by

Carl Budtz-Joergensen, Peter T. Guenther, Alan B. Smith, and James F. Whalen

September 1981

ARGONNE NATIONAL LABORATORY,
ARGONNE, ILLINOIS 60439, U.S.A.

NUCLEAR DATA AND MEASUREMENTS SERIES

ANL/NDM-61

FAST-NEUTRON TOTAL AND SCATTERING CROSS SECTIONS OF ^{58}Ni[a]

by

Carl Budtz-Jørgensen[b], Peter T. Guenther, Alan B. Smith and James F. Whalen

September 1981

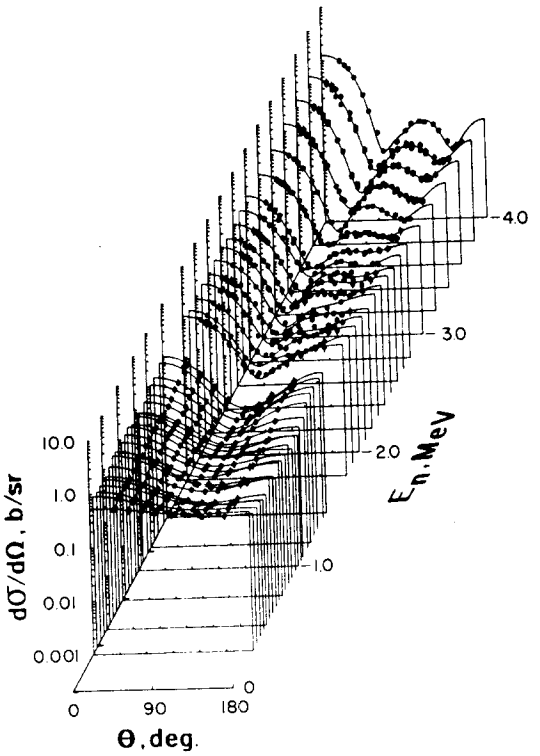

U of C-AUA-USDOE

ARGONNE NATIONAL LABORATORY,
ARGONNE, ILLINOIS 60439, U.S.A.

The facilities of Argonne National Laboratory are owned by the United States Government. Under the terms of a contract (W-31-109-Eng-38) between the U. S. Department of Energy, Argonne Universities Association and The University of Chicago, the University employs the staff and operates the Laboratory in accordance with policies and programs formulated, approved and reviewed by the Association.

MEMBERS OF ARGONNE UNIVERSITIES ASSOCIATION

The University of Arizona
Carnegie-Mellon University
Case Western Reserve University
The University of Chicago
University of Cincinnati
Illinois Institute of Technology
University of Illinois
Indiana University
Iowa State University
The University of Iowa
Kansas State University
The University of Kansas
Loyola University
Marquette University
Michigan State University
The University of Michigan
University of Minnesota
University of Missouri
Northwestern University
University of Notre Dame
The Ohio State University
Ohio University
The Pennsylvania State University
Purdue University
Saint Louis University
Southern Illinois University
The University of Texas at Austin
Washington University
Wayne State University
The University of Wisconsin

NOTICE

This report was prepared as an account of work sponsored by the United States Government. Neither the United States nor the United States Department of Energy, nor any of their employees, nor any of their contractors, subcontractors, or their employees, makes any warranty, express or implied, or assumes any legal liability or responsibility for the accuracy, completeness or usefulness of any information, apparatus, product or process disclosed, or represents that its use would not infringe privately-owned rights. Mention of commercial products, their manufacturers, or their suppliers in this publication does not imply or connote approval or disapproval of the product by Argonne National Laboratory or the U. S. Department of Energy.

ANL/NDM-61

FAST-NEUTRON TOTAL AND SCATTERING CROSS SECTIONS OF ^{58}Ni[a]

by

Carl Budtz-Jørgensen[b], Peter T. Guenther, Alan B. Smith and James F. Whalen

September 1981

[a]This work supported by the U.S. Department of Energy.

[b]Visiting scientist from the Central Bureau for Nuclear Measurements, Geel, Belgium.

Applied Physics Division
Argonne National Laboratory
9700 South Cass Avenue
Argonne, Illinois 60439
USA

NUCLEAR DATA AND MEASUREMENTS SERIES

The Nuclear Data and Measurements Series presents results of studies in the field of microscopic nuclear data. The primary objective is the dissemination of information in the comprehensive form required for nuclear technology applications. This Series is devoted to: a) measured microscopic nuclear parameters, b) experimental techniques and facilities employed in measurements, c) the analysis, correlation and interpretation of nuclear data, and d) the evaluation of nuclear data. Contributions to this Series are reviewed to assure technical competence and, unless otherwise stated, the contents can be formally referenced. This Series does not supplant formal journal publication but it does provide the more extensive information required for technological applications (e.g., tabulated numerical data) in a timely manner.

OTHER ISSUES IN THE ANL/NDM SERIES ARE:

ANL/NDM-1 Cobalt Fast Neutron Cross Sections-Measurement and Evaluation by P. T. Guenther, P. A. Moldauer, A. B. Smith, D. L. Smith and J. F. Whalen, July 1973.

ANL/NDM-2 Prompt Air-Scattering Corrections for a Fast-Neutron Fission Detector: $E_n \leq 5$ MeV by Donald L. Smith, September 1973.

ANL/NDM-3 Neutron Scattering from Titanium; Compound and Direct Effects by E. Barnard, J. deVilliers, P. Moldauer, D. Reitmann, A. Smith and J. Whalen, October 1973.

ANL/NDM-4 ^{90}Zr and ^{92}Zr; Neutron Total and Scattering Cross Sections by P. Guenther, A. Smith and J. Whalen, July 1974.

ANL/NDM-5 Delayed Neutron Data - Review and Evaluation by Samson A. Cox, April 1974.

ANL/NDM-6 Evaluated Neutronic Cross Section File for Niobium by R. Howerton, Lawrence Livermore Laboratory and A. Smith, P. Guenther and J. Whalen, Argonne National Laboratory, May 1974.

ANL/NDM-7 Neutron Total and Scattering Cross Sections of Some Even Isotopes of Molybdenum and the Optical Model by A. B. Smith, P. T. Guenther and J. F. Whalen, June 1974.

ANL/NDM-8 Fast Neutron Capture and Activation Cross Sections of Niobium Isotopes by W. P. Poenitz, May 1974.

ANL/NDM-9 Method of Neutron Activation Cross Section Measurement for E_n = 5.5-10 MeV Using the D(d,n)He-3 Reaction as a Neutron Source by D. L. Smith and J. W. Meadows, August 1974.

ANL/NDM-10 Cross Sections for (n,p) Reactions on ^{27}Al, $^{46,47,48}Ti$, $^{54,56}Fe$, ^{58}Ni, ^{59}Co and ^{64}Zn from Near Threshold to 10 MeV by Donald L. Smith and James W. Meadows, January 1975.

ANL/NDM-11 Measured and Evaluated Fast Neutron Cross Sections of Elemental Nickel by P. Guenther, A. Smith, D. Smith and J. Whalen, Argonne National Laboratory and R. Howerton, Lawrence Livermore Laboratory, July 1975.

ANL/NDM-12 A Spectrometer for the Investigation of Gamma Radiation Produced by Neutron-Induced Reactions by Donald L. Smith, April 1975.

ANL/NDM-13 Response of Several Threshold Reactions in Reference Fission Neutron Fields by Donald L. Smith and James W. Meadows, June 1975.

ANL/NDM-14 Cross Sections for the $^{66}Zn(n,p)^{66}Cu$, $^{113}In(n,n')^{113m}In$ and $^{115}In(n,n')^{115m}In$ Reactions from Near Threshold to 10 MeV by Donald L. Smith and James W. Meadows, July 1975.

ANL/NDM-15 Radiative Capture of Fast Neutrons in ^{165}Ho and ^{181}Ta by W. P. Poenitz, June 1975.

ANL/NDM-16 Fast Neutron Excitation of the Ground-State Rotational Band of ^{238}U by P. Guenther, D. Havel and A. Smith, September 1975.

ANL/NDM-17 Sample-Size Effects in Fast-Neutron Gamma-Ray Production Measurements: Solid-Cylinder Samples by Donald L. Smith, September 1975.

ANL/NDM-18 The Delayed Neutron Yield of ^{238}U and ^{241}Pu by J. W. Meadows January 1976.

ANL/NDM-19 A Remark on the Prompt-Fission-Neutron Spectrum of ^{252}Cf by P. Guenther, D. Havel, R. Sjoblom and A. Smith, March 1976.

ANL/NDM-20 Fast-Neutron-Gamma-Ray Production from Elemental Iron: $E_n \lesssim$ 2 MeV by Donald L. Smith, May 1976.

ANL/NDM-21 Note on the Experimental Determination of the Relative Fast-Neutron Sensitivity of a Hydrogenous Scintillator by A. Smith, P. Guenther and R. Sjoblom, June 1976.

ANL/NDM-22 Note on Neutron Scattering and the Optical Model Near A=208 by P. Guenther, D. Havel and A. Smith, September 1976.

ANL/NDM-23 Remarks Concerning the Accurate Measurement of Differential Cross Sections for Threshold Reactions Used in Fast-Neutron Dosimetry for Fission Reactors by Donald L. Smith, December 1976.

ANL/NDM-24 Fast Neutron Cross Sections of Vanadium and an Evaluated Neutronic File by P. Guenther, D. Havel, R. Howerton, F. Mann, D. Smith, A. Smith and J. Whalen, May 1977.

ANL/NDM-25 Determination of the Energy Scale for Neutron Cross Section Measurements Employing a Monoenergetic Accelerator by J. W. Meadows, January 1977.

ANL/NDM-26 Evaluation of the IN-115(N,N')IN-115M Reaction for the ENDF/B-V Dosimetry File by Donald L. Smith, December 1976.

ANL/NDM-27 Evaluated (n,p) Cross Sections of ^{46}Ti, ^{47}Ti and ^{48}Ti by C. Philis and O. Bersillon, Bruyeres-le-Chatel, France and D. Smith and A. Smith, Argonne National Laboratory, January 1977.

ANL/NDM-28 Titanium-II: An Evaluated Nuclear Data File by C. Philis, Centre d'Etudes de Bruyéres-le-Châtel, R. Howerton, Lawrence Livermore Laboratory and A. B. Smith, Argonne National Laboratory, June 1977.

ANL/NDM-29 Note on the 250 keV Resonance in the Total Neutron Cross Section of ^{6}Li by A. B. Smith, P. Guenther, D. Havel and J. F. Whalen, June 1977.

ANL/NDM-30 Analysis of the Sensitivity of Spectrum-Average Cross Sections to Individual Characteristics of Differential Excitation Functions by Donald L. Smith, March 1977.

ANL/NDM-31 Titanium-I: Fast Neutron Cross Section Measurements by P. Guenther, D. Havel, A. Smith and J. Whalen, May 1977.

ANL/NDM-32 Evaluated Fast Neutron Cross Section of Uranium-238 by W. Poenitz, E. Pennington, and A. B. Smith, Argonne National Laboratory and R. Howerton, Lawrence Livermore Laboratory, October 1977.

ANL/NDM-33 Comments on the Energy-Averaged Total Neutron Cross Sections of Structural Materials by A. B. Smith and J. F. Whalen, June 1977.

ANL/NDM-34 Graphical Representation of Neutron Differential Cross Section Data for Reactor Dosimetry Applications by Donald L. Smith, June 1977.

ANL/NDM-35 Evaluated Nuclear Data File of Th-232 by J. Meadows, W. Poenitz, A. Smith, D. Smith and J. Whalen, Argonne National Laboratory and R. Howerton, Lawrence Livermore Laboratory, February 1978.

ANL/NDM-36 Absolute Measurements of the $^{233}U(n,f)$ Cross Section Between 0.13 and 8.0 MeV by W. P. Poenitz, April 1978.

ANL/NDM-37 Neutron Inelastic Scattering Studies for Lead-204 by D. L. Smith and J. W. Meadows, December 1977.

ANL/NDM-38 The Alpha and Spontaneous Fission Half-Lives of ^{242}Pu by J. W. Meadows, December 1977.

ANL/NDM-39 The Fission Cross Section of ^{239}Pu Relative to ^{235}U from 0.1 to 10 MeV by J. W. Meadows, March 1978.

ANL/NDM-40 Statistical Theory of Neutron Nuclear Reactions by P. A. Moldauer, February 1978.

ANL/NDM-41 Energy-Averaged Neutron Cross Sections of Fast-Reactor Structural Materials by A. Smith, R. McKnight and D. Smith, February 1978.

ANL/NDM-42 Fast Neutron Radiative Capture Cross Section of ^{232}Th by W. P. Poenitz and D. L. Smith, March 1978.

ANL/NDM-43 Neutron Scattering from ^{12}C in the Few-MeV Region by A. Smith, R. Holt and J. Whalen, September 1978.

ANL/NDM-44 The Interaction of Fast Neutrons with ^{60}Ni by A. Smith, P. Guenther, D. Smith and J. Whalen, January 1979.

ANL/NDM-45 Evaluation of $^{235}U(n,f)$ between 100 KeV and 20 MeV by W. P. Poenitz, July 1979.

ANL/NDM-46 Fast-Neutron Total and Scattering Cross Sections of ^{107}Ag in the MeV Region by A. Smith, P. Guenther, G. Winkler and J. Whalen, January 1979.

ANL/NDM-47 Scattering of MeV Neutrons from Elemental Iron by A. Smith and P. Guenther, March 1979.

ANL/NDM-48 ^{235}U Fission Mass and Counting Comparison and Standardization by W. P. Poenitz, J. W. Meadows and R. J. Armani, May 1979.

ANL/NDM-49 Some Comments on Resolution and the Analysis and Interpretation of Experimental Results from Differential Neutron Measurements by Donald L. Smith, November 1979.

ANL/NDM-50 Prompt-Fission-Neutron Spectra of ^{233}U, ^{235}U, ^{239}Pu and ^{240}Pu Relative to that of ^{252}Cf by A. Smith, P. Guenther, G. Winkler and R. McKnight, September 1979.

ANL/NDM-51 Measured and Evaluated Neutron Cross Sections of Elemental Bismuth by A. Smith, P. Guenther, D. Smith and J. Whalen, April 1980.

ANL/NDM-52 Neutron Total and Scattering Cross Sections of ^{6}Li in the Few MeV Region by P. Guenther, A. Smith and J. Whalen, February 1980.

ANL/NDM-53 Neutron Source Investigations in Support of the Cross Section at the Argonne Fast-Neutron Generator by James W. Meadows and Donald L. Smith, May 1980.

ANL/NDM-54 The Nonelastic-Scattering Cross Sections of Elemental Nickel by A. B. Smith, P. T. Guenther and J. F. Whalen, June 1980.

ANL/NDM-55 Thermal Neutron Calibration of a Tritium Extraction Facility using the $^{6}Li(n,t)^{4}He/^{197}Au(n,\gamma)^{198}Au$ Cross Section Ratio for Standardization by M. M. Bretscher and D. L. Smith, August 1980.

ANL/NDM-56 Fast-neutron Interactions with ^{182}W, ^{184}W and ^{186}W by P. T. Guenther, A. B. Smith and J. F. Whalen, June 1981.

ANL/NDM-57 The Total, Elastic- and Inelastic-Scattering of Fast-Neutron Cross Sections of Natural Chromium by Peter T. Guenther, Alan B. Smith and James F. Whalen, January 1981.

ANL/NDM-58 Review of Measurement Techniques for the Neutron Capture Process, Wolfgang P. Poenitz, (to be published).

ANL/NDM-59 Review of the Importance of the Neutron Capture Process in Fission Reactors, Wolfgang P. Poenitz, (to be published).

ANL/NDM-60 Neutron Capture Activation Cross Sections of $^{94,96}Zr$, $^{98,100}Mo$, and $^{110,114,116}Cd$ at Thermal and 30 keV Energy, John M. Wyrick and Wolfgang P. Poenitz, (to be published).

TABLE OF CONTENTS

	Page
LIST OF FIGURES	vii
LIST OF TABLES	viii
ABSTRACT	ix
I. INTRODUCTION	1
II. EXPERIMENTAL METHODS	2
III. EXPERIMENTAL RESULTS	5
IV. INTERPRETATION	16
V. SUMMARY REMARKS	22
ACKNOWLEDGMENTS	22
REFERENCES	23

LIST OF FIGURES

No.	Title	Page
1.	Neutron total and angle-integrated elastic-scattering cross sections of ^{58}Ni. Data symbols denote the present measured values averaged over 200 keV. Curves indicate the results of model calculations as described in the text	6,7
2.	Differential-elastic-scattering cross sections of ^{58}Ni. The present experimental results, averaged over 200 keV, are indicated by the data points. Curves denote Legendre-polynomial fits to the measured values. The dimensionality is cross section in b/sr and scattering angle in lab. deg	8,9
3.	Differential cross sections for the excitation of the 1.458 MeV level in ^{58}Ni. The present experimental results, averaged over 200 keV, are indicated by data symbols. The results of least-square Legendre-polynomial fits to the data are indicated by curves. The dimensionality is cross section in b/sr and scattering angle in lab. deg	12,13
4.	Angle-integrated neutron inelastic-scattering cross sections of ^{58}Ni. 200 keV averages of the present experimental results are indicated by data points. Heavy curves denote the results of spherical (SPH) and deformed (DEF) model calculations as discussed in the text. Light curves indicate values implied by ENDF/B-V. The energies of the corresponding excited levels are numerically given in MeV	14,15
5.	Differential neutron elastic-scattering cross sections of ^{58}Ni. 200 keV averages of the present measured values are indicated by data symbols. Curves denote the results of spherical model calculations as described in the text. The dimensionality is cross section in b/sr and scattering angle in lab. deg	18,19
6.	Differential elastic- and inelastic- (E_x = 1.458 MeV) scattering cross sections of ^{58}Ni obtained at 2.5 MeV (lower) and 3.5 MeV (upper). Experimental values are denoted by data symbols. Curves denote the results of spherical (plain curves) and deformed (with "tick" marks) model calculations. Dimensionality is b/sr and scattering angle in lab. deg	20,21

LIST OF TABLES

No.	Title	Page
I.	Comparison of Observed and Reported Levels in ^{58}Ni.....	25
II.	Spherical Optical-potential Parameters.....	26

FAST-NEUTRON TOTAL AND SCATTERING CROSS SECTIONS OF ^{58}Ni[a]

by

Carl Budtz-Jørgensen[b], Peter T. Guenther, Alan B. Smith
and James F. Whalen

Applied Physics Division
Argonne National Laboratory
9700 South Cass Avenue
Argonne, Illinois 60439

ABSTRACT

Neutron total cross sections of ^{58}Ni were measured at 25 keV intervals from 0.9 to 4.5 MeV with 50-100 keV resolutions. Attention was given to self-shielding corrections to the observed total cross sections. Differential elastic- and inelastic-scattering cross sections were measured at 50 keV intervals from 1.35 to 4.0 MeV with 50-100 keV resolutions. Inelastic excitation of levels at 1.458 ± 0.009, 2.462 ± 0.010, 2.791 ± 0.015, 2.927 ± 0.012 and 3.059 ± 0.025 MeV was observed. The experimental results were interpreted in terms of optical-statistical and coupled-channels models. A spherical optical-statistical model was found generally descriptive of an energy-average of the experimental results. However, detailed considerations suggested significant contributions from direct-vibrational interactions, particularly associated with the excitation of the first 2+ level.

[a]This work supported by the U.S. Department of Energy.

[b]Visiting scientist from the Central Bureau for Nuclear Measurements, Geel, Belgium.

I. INTRODUCTION

Nickel is an important constituent of radiation- and heat-resistant alloys, such as stainless steel, which are widely used in fission- and fusion-energy systems. Thus the interaction of fast neutrons with elemental nickel is of considerable applied importance. The desired accuracies of the elemental fast-neutron-scattering cross sections are ≈5% [1]. The measurement of scattering cross sections to such accuracies is most promising when undertaken on an isotopic basis. The natural element consists of ^{58}Ni (68.3%), ^{60}Ni (26.1%), ^{61}Ni (1.1%), ^{62}Ni (3.6%) and ^{64}Ni (0.9%). Studies of the interaction of fast neutrons with ^{60}Ni and with elemental nickel have recently been reported by this Group [2,3]. The present work is an extension of the previous efforts to ^{58}Ni with the objective of obtaining precise neutron total and scattering cross sections for the element over an energy range of ≈1 to 4 MeV.

The fast-neutron interaction with ^{58}Ni is a mixture of compound-nucleus and direct processes. The resonance behavior of the compound-nucleus contribution is difficult to resolve experimentally in the present energy range. Moreover, most applications do not utilize high-resolution information in this energy range and most of physical interpretations are based upon energy-averaged models. Thus it was the intent of the present work to obtain energy-averaged total and scattering cross sections to an intermediate-energy resolution consistent with most of the application usage and with energy-averaged model concepts. The latter, in the form of optical-statistical and coupled-channels models, were employed in the physical interpretation of the measured values with attention to contributions due to resonance fluctuations and to direct-collective-vibrational excitations.

II. EXPERIMENTAL METHODS

A. Measurement Sample

All the measurements employed a single cylindrical sample of metallic nickel 2 cm in diameter and 2 cm long, isotopically enriched to 99.93% atom-percent in ^{58}Ni [4]. The minor-isotope content of the sample was assumed negligible. However, in the course of the scattering measurements it became clear that the sample contained a chemical impurity. The scattered-neutron velocity spectra observed at large angles indicated a carbon contaminate of 1.8 ± 0.2 atom-percent abundance. All the nickel results were corrected for this carbon contamination. The corrections were determined using the results of concurrent measurements of carbon total and scattering cross sections. These corrections introduced a small ($\approx$0.2%) uncertainty in the measured nickel cross sections.

B. Neutron Total Cross Sections

Ideally, the neutron total cross section is readily determined from the observed transmission of neutrons through the sample by means of the expression [5];

$$\sigma(E) = -\frac{1}{\eta} \ln T(E) \quad , \tag{1}$$

where the sample transmission (T) at energy (E) is determined with a resolution (dE) sufficient to resolve the structure in the cross section and η is the area density of nuclei in the sample. In broad-resolution measurements dE may be far coarser than the underlying structure and only an effective cross section is obtained, given by;

$$\sigma_{eff}(E) = -\frac{1}{\eta} \ln \langle T \rangle_{E,dE} \quad . \tag{2}$$

Due to the underlying structure, the difference between the effective cross section and the true energy-averaged cross section (σ_o) can be large as emphasized in Refs. 6 and 7. For sufficiently small samples Eq. 2 reduces to;

$$\sigma_{eff}(E) = \sigma_o(E) - \alpha(E) \cdot \eta \quad , \tag{3}$$

where α is the variance of the total cross section. Hence, σ_{eff} can be obtained by linearly extrapolating results measured with varying sample thicknesses to the zero-thickness limit. Such an experimental procedure was not attractive in the present case as the necessary range of ^{58}Ni sample thicknesses was not available. An alternate approach uses dE values smaller

than the fluctuations of the underlying structure and thus provides the true cross sections of Eq. 1 which can be subsequently averaged over the desired energy increment. This high-resolution experimental alternative was examined using the pseudo-white source technique. Neutron bursts of ≈1 nsec duration with an energy spread of 100 to 200 keV were obtained by bombarding an appropriate lithium-metal target with a pulsed proton beam. A proton-recoil-scintillation neutron detector was placed 37 m from the neutron source at the end of an evacuated flight tube oriented at a zero-degree source-reaction angle. The transmission sample was placed ≈1 m from the source on the source-detector axis. The overall time response of the measurement system was ≈2.2 nsec as determined by observation of the narrow carbon resonance at ≈2.8 MeV. Thus the velocity resolution of the system was ≈0.06 nsec/m. With this arrangement a series of elemental nickel measurements were made using sample thicknesses in the range 0.06 to 0.4 at/b. The measurements extended over the neutron energy range 0.8 to 1.5 MeV. Cross sections were determined from the observed transmissions using Eq. 1 and averaged over a 50 keV energy increment. These energy-averaged results were strongly dependent on sample thickness. Thus it was concluded that the energy resolutions were far short of those necessary for determining the ^{58}Ni neutron total cross sections free of self-shielding perturbations. It is noted that the above resolutions are comparable to those employed in a number of white-source measurements of the nickel total cross sections [8,9]. Thus some of the previously reported neutron total cross sections may suffer from self-shielding perturbations, particularly as relatively thick samples were frequently employed.

In view of the above problems, effective broad-resolution ^{58}Ni neutron total cross sections were measured and reduced to true values using self-shielding correction factors determined from elemental nickel measurements employing a wide range of sample thicknesses. In doing so it was assumed that the cross section variances of the nickel isotopes were identical in magnitude and that the isotopic resonance structure was uncorrelated. With these assumptions it follows that;

$$\sigma_{eff}^{Ni} = \sigma_{o}^{Ni} - n \left(\sum_{i} a_i^2\right)\alpha^{58} \quad , \tag{4}$$

where a_i are the effective abundances of the nickel isotopes. The measurements were made using the total cross section apparatus at the Argonne Fast-neutron Generator. This measurement apparatus and the associated measurement technique are amply described elsewhere [6,7]. In addition to the ^{58}Ni sample, five elemental nickel samples were used ranging in thickness from 0.06 to 0.4 at/b. The neutron total cross sections of carbon were determined concurrently to assure the proper functioning of the measurement system. The energy scale was determined to within ≈10 keV by observations of well known resonances in carbon, silicon and sulfur with resolutions of ≈5 keV. Background and dead-time corrections were treated as described in Refs. 6 and 7. Inscattering effects were negligible.

C. Neutron Scattering Measurements

The neutron scattering measurements were made using the Argonne National Laboratory 10-angle, pulsed-beam, time-of-flight apparatus [10]. The neutron source was the $^{7}Li(p,n)^{7}Be$ reaction, pulsed for durations of $\approx$1 nsec at a repetition rate of 2 MHz. The scattering samples were placed $\approx$13 cm from the source at a zero-degree source-reaction angle. Ten proton-recoil-scintillation detectors viewed the sample through $\approx$5 m flight paths, distributed over the angular range 20 to 160 degs. The source intensity was monitored using an independent time-of-flight system. The relative energy-dependent response of each of the neutron detectors was determined by observing neutrons emitted from the spontaneous fission of ^{252}Cf [11]. These ten independent response functions were correlated by observing neutrons scattered from carbon at a selected angle, nominally 35 degrees, with each detector. The absolute response of the correlated system was then determined by measuring the relative differential-elastic-scattering cross sections of carbon, angle-integrating these distributions and comparing the resulting angle-integrated values with the well known carbon neutron total cross sections [12,13]. At the energies of the present experiments the neutron elastic-scattering and total cross sections of carbon are essentially identical. These calibration procedures implied that the measured scattering cross sections were determined relative to the neutron total cross section of elemental carbon. More details of the calibration procedures are given in Ref. 12. The uncertainties associated with the detector calibrations were; $\lesssim$3% due to the carbon-calibration measurements, $\lesssim$2% due to the uncertainty of the reference carbon neutron total cross section, and $\lesssim$3% due to the ^{252}Cf relative-response determinations. Thus the overall detector-calibration uncertainties were conservatively $\lesssim$5%. All the experimental results were corrected for multiple-event, angular-resolution and sample attenuation perturbations using analytical and Monte-Carlo procedures as described in Ref. 10. The uncertainty in the measured cross sections due to these correction procedures was $\lesssim$1%.

III. EXPERIMENTAL RESULTS

A. Neutron Total Cross Sections

The ^{58}Ni and elemental nickel measurements were made concurrently at ≈25 keV intervals from 0.9 to 4.5 MeV with energy resolutions of 50 to 100 keV. The resulting ^{58}Ni cross sections were initially corrected for the small carbon impurity, noted above, and both ^{58}Ni and elemental nickel cross sections were averaged over 200 keV energy increments using a "running average" procedure. The ^{58}Ni correction factor (α^{58} of Eq. 4) was obtained by least-square fitting the results obtained from the five elemental nickel samples with Eq. 4. No significant deviation from linearity of cross section dependence on sample thickness was observed but the self-shielding correction factors were strongly energy dependent varying from ≈10% at 1.0 MeV, to ≈5% at 1.5 MeV, ≈3% at 2.0 MeV and finally becoming negligible above ≈3.0 MeV. Considering the assumptions underlying Eq. 4, it was estimated that the correction-factor uncertainties were ≲30%. Systematic deviation of the correction factors from a linear dependence on sample thickness would tend to increase their magnitudes [14]. The corrected ^{58}Ni neutron total cross sections are shown in Fig. 1. The statistical uncertainties (≲1%) were small compared with those due to the above self-shielding correction factors below several MeV. Even with the broad 200 keV averages of Fig. 1, residual fluctuations are evident particularly below ≈2.0 MeV.

Previously reported comparable neutron total cross sections of ^{58}Ni are sparse. Thibault [15] gives a value of 3.08 ± 0.1b at 2.7 MeV. This result is somewhat smaller than the results of the present work but comparisons of isolated values in the context of the evident fluctuations can be deceptive. The present results are in reasonable agreement (≲5%) with the broad-resolution elemental-nickel values recently reported from this Group [3] as should be expected from the prominent natural abundance of the ^{58}Ni isotope.

B. Neutron Elastic Scattering

Neutron elastic-scattering cross sections were measured at intervals of ≈50 keV from 1.35 to 4.0 MeV with incident-energy resolutions of ≈50-100 keV. The measurements were made at ten scattering angles distributed between 20 and 160 degrees. The scattering angles were known to ≲1.0 degree. The statistical accuracies of the individual differential-cross-section values was ≲3% (frequently less than 1%). Thus the overall differential-cross-section uncertainties were ≲5% and predominately due to the detector-calibration factors outlined above.

Despite the fact that the measurements were intentionally made with broad resolutions, the scattered-neutron angular distributions displayed relatively large energy-dependent variations reflecting the underlying fluctuations of the ^{58}Ni compound-nucleus cross section. Thus the measured data was averaged over 200-keV energy intervals in order to smooth the fluctuations and obtain energy-average results consistent with optical-statistical and coupled-channels models. The resulting energy-averaged distributions are illustrated in Fig. 2.

Fig. 1. Neutron total and angle-integrated elastic-scattering cross sections of ^{58}Ni. Data symbols denote the present measured values averaged over 200 keV. Curves indicate the results of model calculations as described in the text.

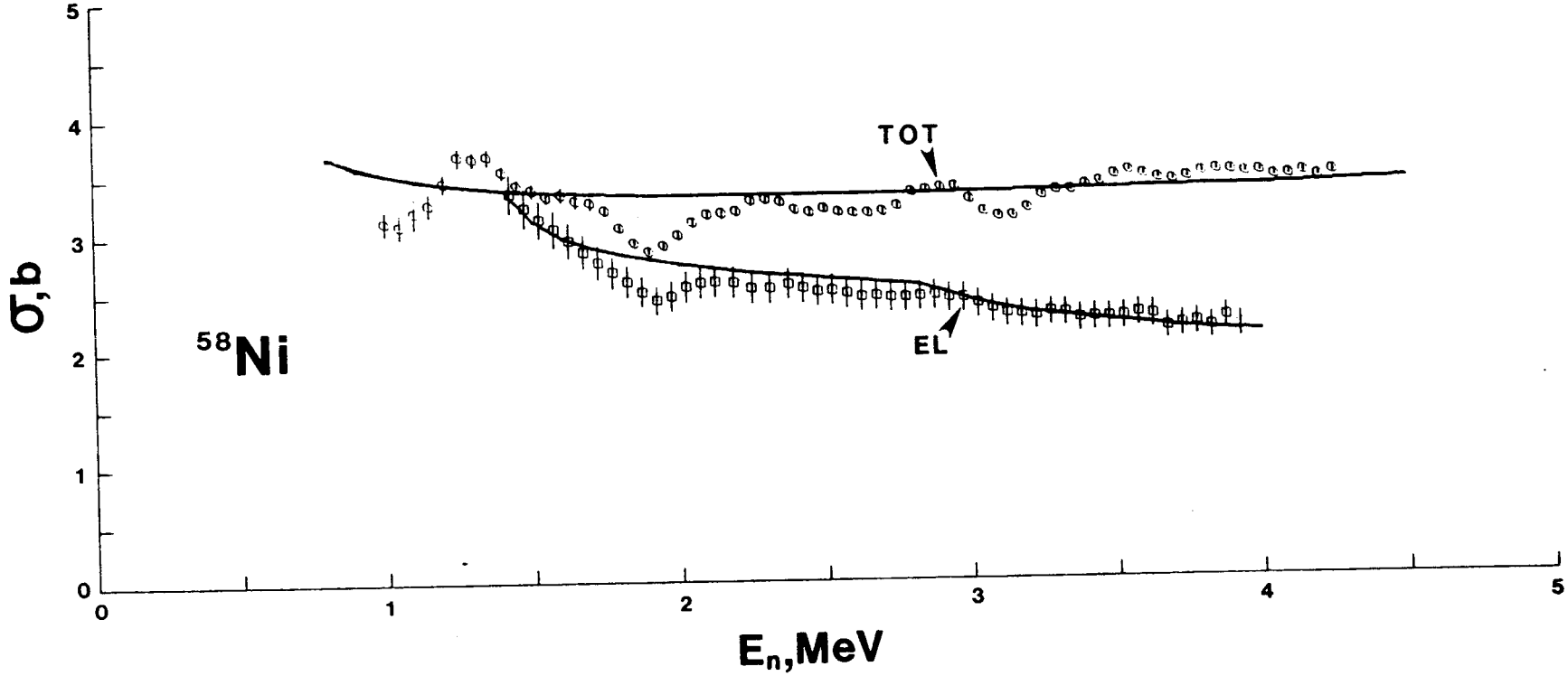

Fig. 1

Fig. 2. Differential-elastic-scattering cross sections of ^{58}Ni. The present experimental results, averaged over 200 keV, are indicated by the data points. Curves denote Legendre-polynomial fits to the measured values. The dimensionality is cross section in b/sr and scattering angle in lab-deg.

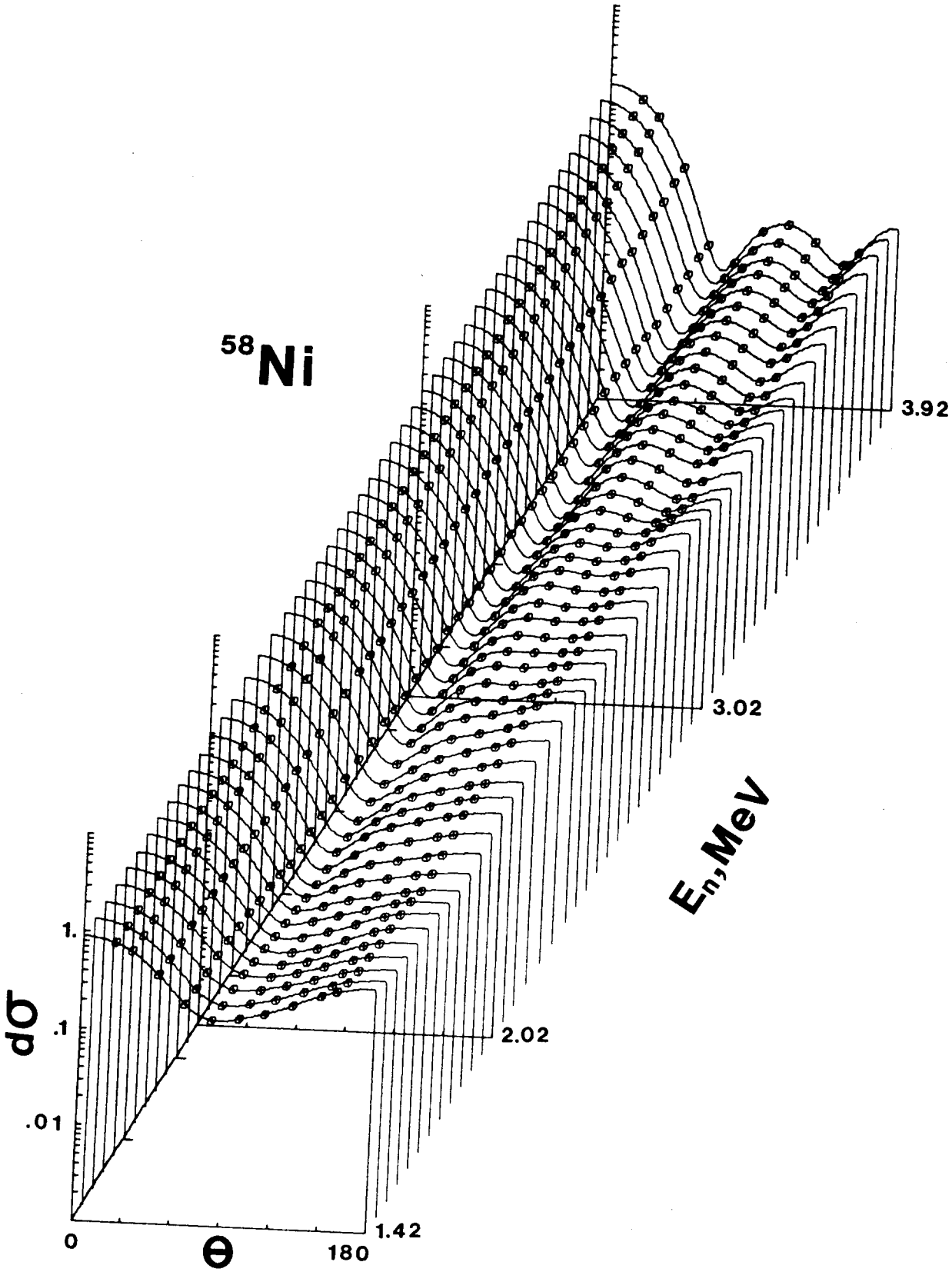

Fig. 2

These distributions were least-squares fitted with a 6th-order Legendre-polynomial series in order to obtain the angle-integrated elastic-scattering cross sections shown in Fig. 1. The accuracies of the angle-integrated values were conservatively estimated to be $\lesssim$5%. The angle-integrated results were consistent with the above neutron total cross sections. The structures of the two cross sections are similar, particularly in the region of the minimum at 1.9 MeV. At the low-energy extreme of the elastic-scattering results, below the inelastic-scattering threshold, the measured neutron total and elastic-scattering cross sections agree to well within the experimental uncertainties, as it should be, since the non-elastic cross section in this region is very small.

There are few previously reported ^{58}Ni elastic-scattering results comparable with those of the present work. Rodgers et al. [16] have reported elastic-scattering cross sections at 2.33 and 2.9 MeV. The lower-energy result of Ref. 16 agrees to within 10% with the present work but the higher-energy value is discrepant.

C. Neutron Inelastic Scattering

The differential elastic- and inelastic-scattering measurements were made concurrently. Generally, inelastic-scattering observations were accepted for analysis if the scattered-neutron energy exceeded 0.8 MeV. Observation of neutrons of lower energies was felt to be unreliable due to rapidly changing response functions of some of the detectors $\lesssim$0.8 MeV. Five inelastic-neutron groups were observed corresponding to the excitation of the levels given in Table I. The excitation energies were determined from measured incident-neutron energies, flight times and flight paths. The uncertainties of the derived level energies were defined as RMS values resulting from a number of observations. The observed levels were consistent with those reported in the literature [17] as shown in Table I. The identification is unique except in the case of the observed 2.927 MeV level which was attributed to a reported doublet with a spacing smaller than the resolutions employed in the present experiments.

The inelastic-scattering angular distributions display the same type of fluctuations as the elastic-scattering above. Thus they were averaged over 200 keV energy intervals to obtain reasonable energy-averaged values. The resulting energy-averaged distributions behaved in a relatively smooth manner as illustrated by the excitation of the 1.458 MeV level shown in Fig. 3. Generally, the observed inelastic angular distributions were symmetric about 90 degs in the center-of-mass system. An exception was the excitation of the 1.458 MeV level where there was an increasing deviation from symmetry with energy toward a systematic forward-angle bias as illustrated in Fig. 3.

The angle-integrated inelastic-scattering cross sections were deduced from the observed angular distributions by fitting the measured values with low-order Legendre series in a manner anologous to that employed in the analysis of the elastic-scattering distributions. The uncertainties of the resulting angle-integrated cross sections ranged from $\approx$5%, in the prominent

and well resolved cases, to ≈20% for less favorable cases associated with small cross sections. The origins of the uncertainties were essentially as defined above for elastic scattering with larger statistical uncertainties in some cases. The inelastic angle-integrated cross sections are summarized in Fig. 4. The most prominent of these are due to the excitation of the 1.458 MeV one-phonon vibrational level. The cross sections for this component are consistent with the above neutron total and elastic-scattering cross sections at energies below the second inelastic-scattering threshold at ≈2.5 MeV. The minimum observed in the total and elastic-scattering cross sections at ≈1.9 MeV is prominently reflected in the cross section for the excitation of the 1.458 MeV level as expected since the latter cross section is essentially proportional to the fluctuating compound-nucleus cross section. More generally, the sum of the present measured inelastic-scattering cross sections is consistent with the above total and elastic-scattering cross sections.

There is little previously reported ^{58}Ni information directly comparable with the present inelastic-scattering results. Pasechnik et al. [18] have recently reported ^{58}Ni inelastic-scattering cross sections at 2.0, 2.5 and 3.0 MeV. Their results are not in particularly good agreement with those of the present work, particularly with respect to the excitation of the 1.458 level where the differences are as much as ≈30%. This may, in part, be due to the necessity of obtaining the data of Ref. 18 from small figures. There are a number of previously reported (n;n') and (n;n',γ) results obtained with elemental nickel targets as described in Ref. 19. These elemental-nickel results are reasonably summarized in the Evaluated Nuclear Data File, ENDF/B-V [20]. Therefore the relevant inelastic-scattering portions of that File were corrected for isotopic content and compared with the present isotopic values as illustrated in Fig. 4. Above ≈3.0 MeV the present results and those of the File for the excitation of the 1.458 MeV level are in reasonable agreement; at lower energies there are differences amounting to 20% to 30%. Some of these differences are attributable to poor definition of structure by the previously reported data underlying the File but, even in a broad average, there remain 10% to 20% discrepancies. The present results for the inelastic excitation of higher-energy levels are reasonably consistent with those implied by the File with no systematic qualitative differences between the two sets of results.

Fig. 3. Differential cross sections for the excitation of the 1.458 MeV level in ^{58}Ni. The present experimental results, averaged over 200 keV, are indicated by data symbols. The results of least-square Legendre-polynomial fits to the data are indicated by curves. The dimensionality is cross section in b/sr and scattering angle in lab. deg.

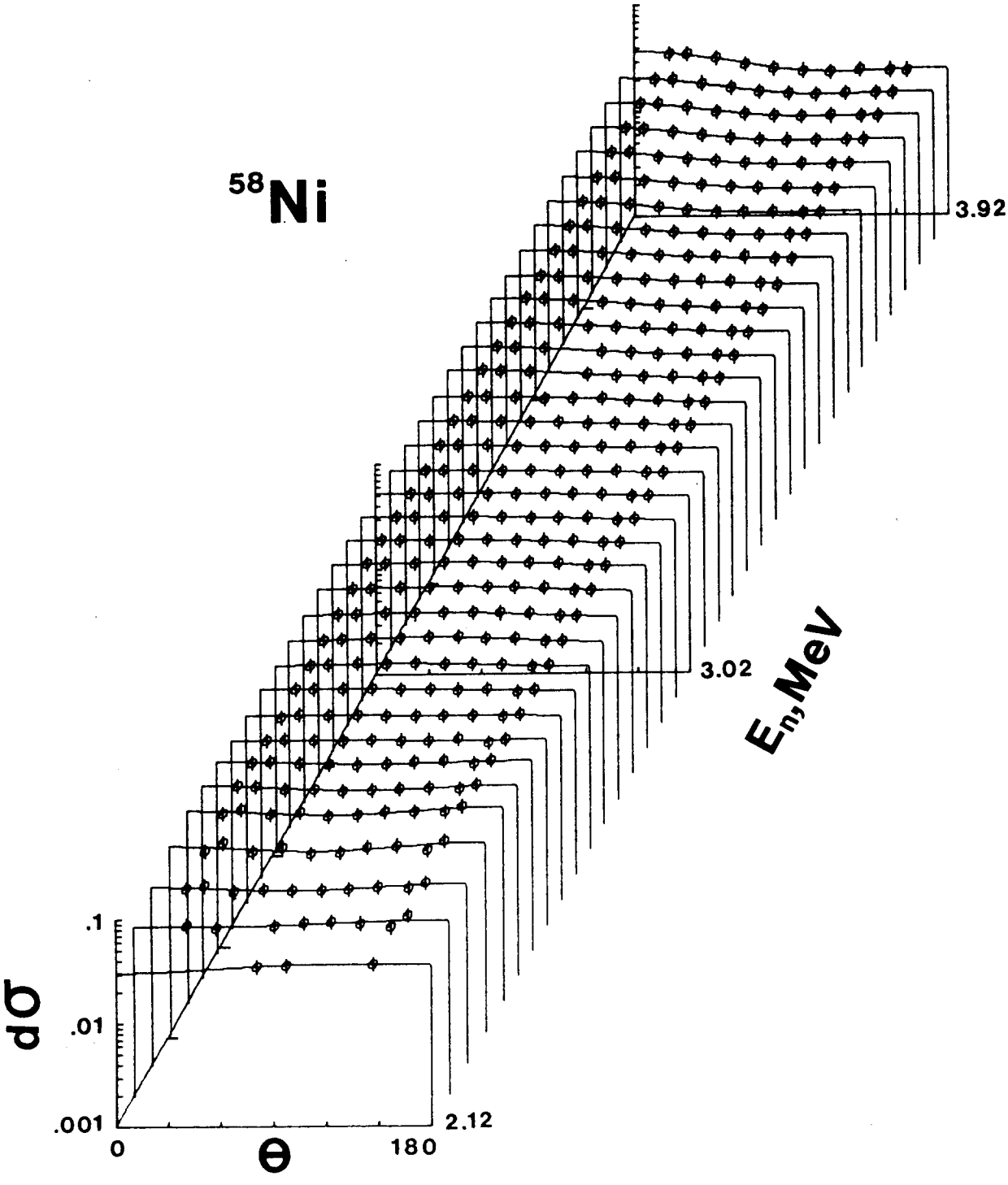

Fig. 3

Fig. 4. Angle-integrated neutron inelastic-scattering cross sections of ^{58}Ni. 200 keV averages of the present experimental results are indicated by data points. Heavy curves denote the results of spherical (SPH) and deformed (DEF) model calculations as discussed in the text. Light curves indicate values implied by ENDF/B-V. The energies of the corresponding observed excited levels are numerically given in MeV.

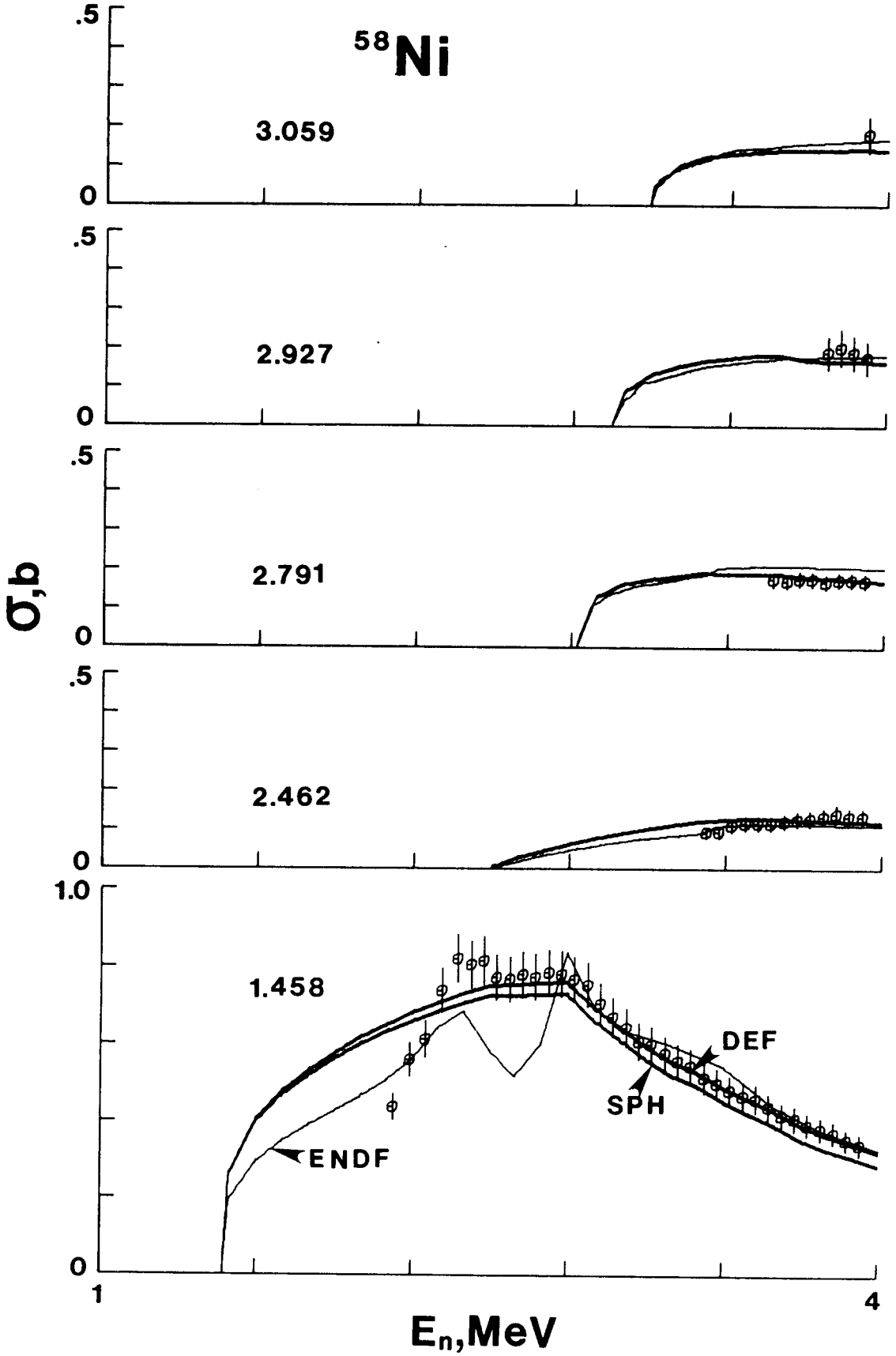

Fig. 4

IV. INTERPRETATION

The above experimental results were examined in the context of optical-statistical [21] and coupled-channels [22] models. The calculations assumed the level structure given in Ref. 17. The spherical calculations employed the code ABAREX [23] and the coupled-channels calculations the code JUPREX [24]. Both codes treat compound-nucleus processes using the Hauser-Feshbach formula [25] as corrected by Moldauer [26]. The initial spherical-model parameters were determined by Chi-square fitting the individual angular distributions of Fig. 3. The fitting procedures concurrently varied the six parameters; real and imaginary strengths, radii and diffusenesses. The spin-orbit potential was kept constant. Though the data base had been averaged over 200 keV there remained residual fluctuations and these were reflected in the parameters resulting from the individual fitting procedures. Thus a simultaneous fit to the entire data base of Fig. 3 was made starting with parameters obtained by averaging those obtained from the individual fits. In this step angular distributions at energies near 2.0 MeV were deleted from the data base as they were in a region of a pronounced minimum of both the total and elastic-scattering cross sections. The energy dependence of the real potential was also adjusted to improve the description of the observed neutron total cross sections. A similar variation of the energy dependence of the imaginary potential did not improve the results significantly. However, in either case the data base does not span a large enough energy range to well define the energy dependence of the optical potential. The final spherical-parameter set is defined in Table II. These parameters are similar to those independently found to be suitable for ^{60}Ni [2] (e.g. the real strengths, Vr^2, differ by $\lesssim$2% and the imaginary strengths, Wa, by $\lesssim$5%). The energy dependence of the present real potential is somewhat larger than commonly employed but consistent with that recently reported for ^{56}Fe [27].

The above spherical potential gives a good description of the observed differential-elastic-scattering cross sections as illustrated in Fig. 5. The differences between measured and calculated values are seldom beyond the experimental uncertainties and were well within the magnitude expected from the residual data fluctuations. The potential also provides a reasonable description of measured total and angle-integrated elastic-scattering cross sections as illustrated in Fig. 1. The fluctuations in the data cannot be portrayed by the energy-averaged model, but the average trends of the data are well represented. This would not be so without the above self-shielding corrections to the observed total cross sections. Indeed, the neglect of such corrections may have been a frequent source of discrepancy between measured and calculated total cross sections in this mass-energy range. The above parameters also provide a reasonable description of the observed inelastic-scattering cross sections as illustrated in Fig. 4. However, the simple spherical model has shortcomings in the inelastic-scattering context. In particular, the excitation of the prominent 1.458 MeV level is systematically under predicted at higher energies and the forward-angle peaking of the corresponding distributions shown in Fig. 3 is inconsistent with a simple compound-nucleus process.

These shortcomings of the spherical calculations are indicative of direct-reaction processes not consistent with the underlying compound-nucleus

assumptions. Indeed, the 1.458 MeV (2+) level is believed to be a one-phonon vibrational state [17] and it is reasonable to expect significant contribution from the direct-vibrational-excitation. This contribution was estimated using coupled-channels calculations assuming the spherical model parameters of Table II and coupling the ground and first-excited states with a strength equivalent to that of the real potential. These assumptions are approximations as the introduction of vibrational coupling will impact upon the choice of the underlying model parameters. However, the direct component was expected to be small and thus could be reasonably treated as a perturbation. With the above assumptions the inelastic-scattering cross sections calculated with the coupled-channels model mitigated the shortcomings of the spherical calculations. Specifically, the calculated excitations of the 1.458 MeV level were larger at higher energies and are in very good agreement with observation as illustrated in Fig. 4. Moreover, at higher energies the corresponding neutron angular distributions were forward peaked and in good agreement with observation as illustrated in Fig. 6. As expected, the direct-reaction contribution decreased with energy and was relatively small at 2.5 MeV. The coupled-channels results were not quite as descriptive of the elastic scattering angular distributions as those obtained with the spherical model, reflecting the need for a more rigorous derivation of the model parameters within the coupled-channels framework. The latter was not attempted due to the relatively limited energy range of the present data base.

Fig. 5. Differential neutron elastic-scattering cross sections of ^{58}Ni. 200 keV averages of the present measured values are indicated by data symbols. Curves denote the results of spherical model calculations as described in the text. The dimensionality is cross section in b/sr and scattering angle in lab. deg.

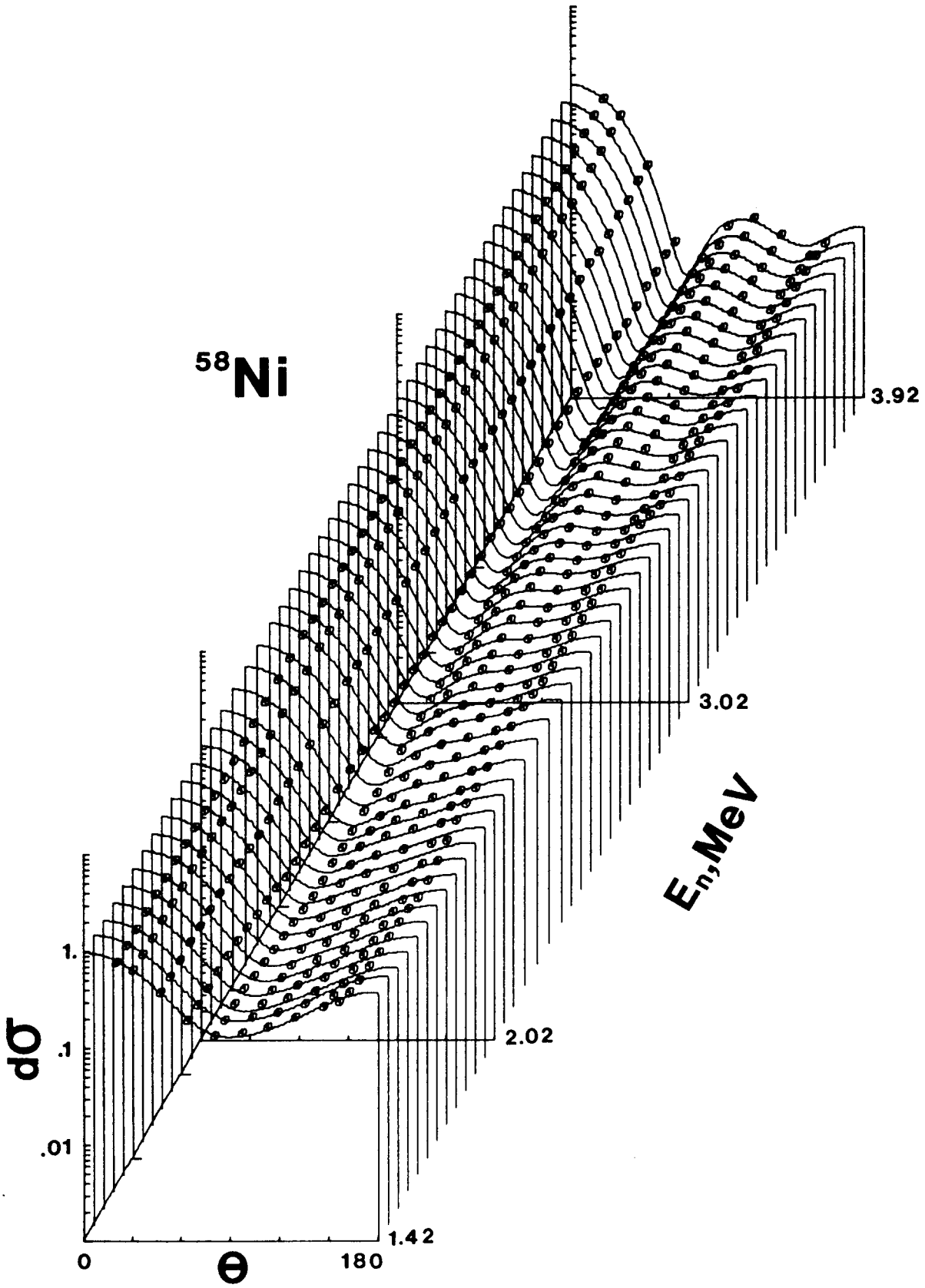

Fig. 5

Fig. 6. Differential elastic- and inelastic- (E_x = 1.458 MeV) scattering cross sections of ^{58}Ni obtained at 2.5 MeV (lower) and 3.5 MeV (upper). Experimental values are noted by data symbols. Curves denote the results of spherical (plain curves) and deformed (with "tick" marks) model calculations. Dimensionality is cross section in b/sr and scattering angle in lab. deg.

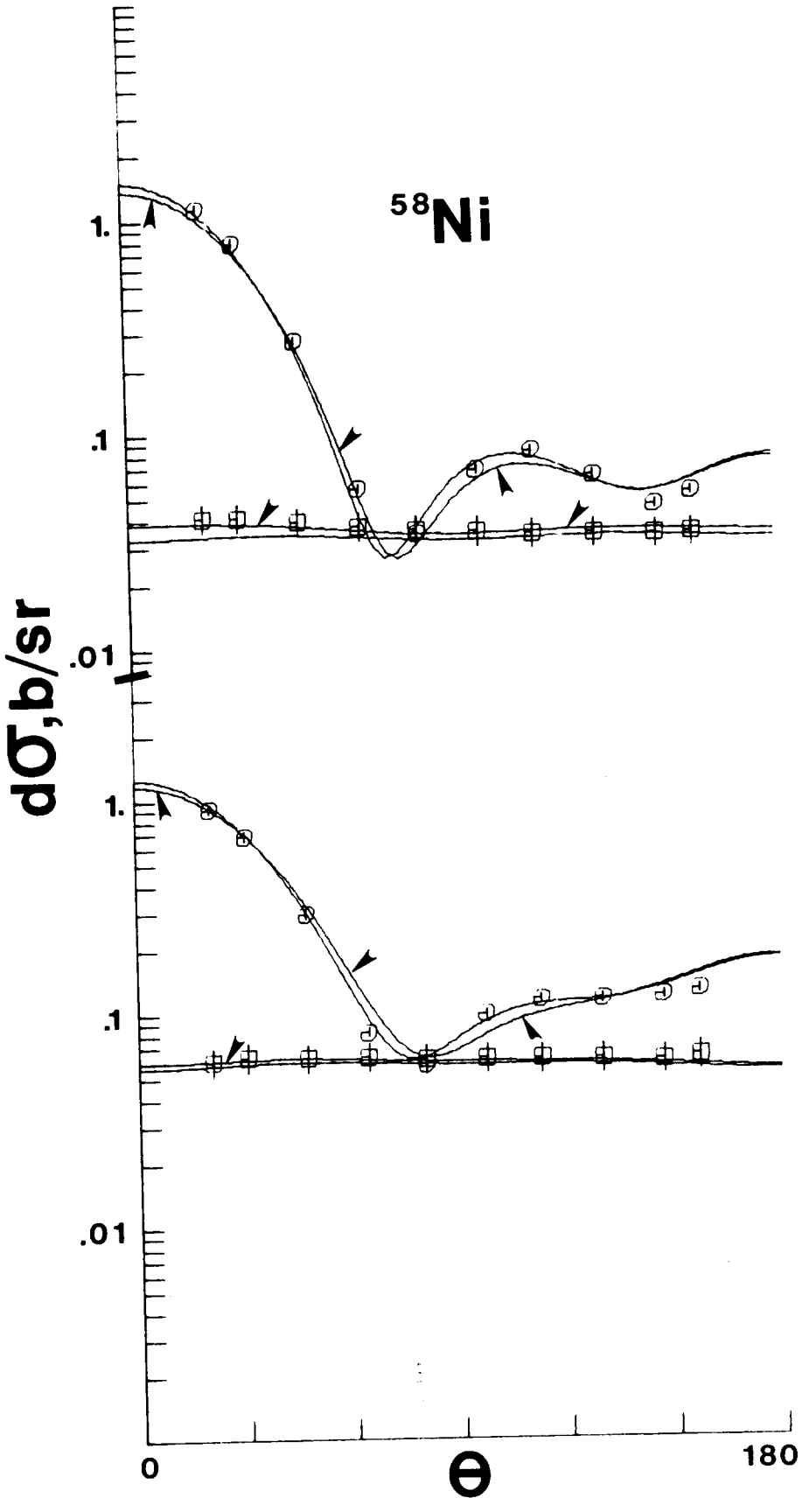

Fig. 6

V. SUMMARY REMARKS

The present measurements define the energy-averaged behavior of the neutron total cross sections of ^{58}Ni from 0.9 to 4.5 MeV to several-percent accuracies. The experimental results are corrected for self-shielding which can amount to $\approx$10% effect on the measured values at the lower energies. These corrections are essential for quantitative cross sections for applied use and model interpretations. It is likely that such corrections have been ignored in many previously reported experimental results in this mass-energy region. The present measurements determine the differential-elastic-scattering cross sections of ^{58}Ni from 1.35 to 4.0 MeV to few-percent accuracies. The results are in sufficient detail to assure a good representation of the energy-averaged behavior of the cross sections suitable for applied use and model interpretations. Inelastic-neutron-scattering cross sections are measured corresponding to the excitation of levels to $\lesssim$3.0 MeV, again with sufficient detail to generally determine the energy-averaged behavior of the cross sections. The observed inelastic-neutron angular-distributions are generally symmetric about 90 deg. However, those associated with the first (2+) level at 1.458 MeV are significantly peaked toward forward angles at higher energies. A simple spherical optical-statistical model, deduced from the measurements, gives a reasonable description of the observed cross sections. However, in detail this simple model does not account for the cross section magnitudes or the inelastic-neutron asymmetries associated with the excitation of the 1.458 MeV level. These shortcomings are alleviated with coupled-channels calculations assuming a direct vibrational excitation of the 1.458 MeV level in addition to the predominant compound-nucleus contribution.

The present experimental results, combined with ^{60}Ni values previously reported from this Group [2], largely fulfill the stated applied needs for elemental nickel scattering data over the energy range 1.4 to 4.0 MeV.

ACKNOWLEDGMENTS

The authors are pleased to acknowledge the advice and assistance of Drs. P. A. Moldauer and W. P. Poenitz.

REFERENCES

1. WRENDA, World Request List for Nuclear Data Measurements, IAEA Report, INDC (SEC)-38/U (1974).

2. A. Smith, P. Guenther, D. Smith and J. Whalen, Nucl. Sci. and Eng., 72, 293(1979).

3. A. Smith, P. Guenther and J. Whalen, Nucl. Sci. and Eng., 77, 110(1981).

   In the course of the present work a minor error in the results of this paper was noted. The substance of the paper is not significantly effected. Revised numerical data has been sent to the National Nuclear Data Center, Brookhaven Natl. Lab.

4. The authors are indebted to E. Kobisk et al., Oak Ridge Natl. Lab., for fabricating the ^{58}Ni sample.

5. D. Miller, Fast Neutron Physics, Vol - II, J. Marion and J. Fowler Eds., Interscience Pub., (1963) New York.

6. A. Smith, P. Guenther and J. Whalen, Argonne Natl. Lab. Report, ANL/NDM-54 (1980).

7. P. Guenther, A. Smith and J. Whalen, Argonne Natl. Lab. Report, ANL/NDM-57 (1981).

8. S. Cierjacks, P. Forti, D. Kopsch, L. Kropp, J. Nebe and H. Unfeld, Karlsruhe Report, KFK-1000 (1968).

9. R. Schwartz, R. Schrack and H. Heaton, Natl. Bureau of Standards Report, NBS-138 (1974).

10. P. T. Guenther, The elastic and inelastic scattering of fast neutrons from the even isotopes of tungsten, Univ. of Illinois Thesis (1977).

11. A. Smith, P. Guenther, and R. Sjoblom, Nucl. Instr. and Methods, 140, 397(1977).

12. A. Smith and P. Guenther, to be published.

13. A. Smith, R. Holt and J. Whalen, Argonne Natl. Lab. Report, ANL/NDM-43 (1978); these carbon values are essentially identical to those of Ref. 20, below.

14. W. Poenitz, J. Whalen and A. Smith, accepted for publication, Nucl. Sci. and Eng., 78, 333(1981).

15. C. Thibault, CEA Report, CEA-R3124 (1967).

16. W. Rodgers, E. Shrader and J. Lindlow, Chicago Operations Office Report, COO-1573, 33(1967).

17. Table of Isotopes, 7th ed., Eds. M. Lederer and V. Shirley, John Wiley and Sons, New York (1978).

18. M. Pasechnik, I. Korzh and E. Mozhzhukhin, Proc. Conf. on Nucl. Cross Sections for Technology, Natl. Bureau of Stds. Pub., NBS-594 (1980).

19. P. Guenther, A. Smith, D. Smith and J. Whalen, Argonne Natl. Lab. Report, ANL/NDM-11 (1975).

20. Brookhaven Natl. Lab. Report, ENDF-102, 2nd ed., R. Kinsey Ed., (1979).

21. P. Hodgson, Nuclear Reactions and Nuclear Structure, Clarendon Press, Oxford (1971).

22. T. Tamura, Rev. Mod. Phys., 37, 679(1965).

23. Computational code ABAREX, private communication from P. Moldauer (1981).

24. Computational code JUPREX, private communication from P. Moldauer (1981).

25. W. Hauser and H. Feshbach, Phys. Rev., 87, 366(1952).

26. P. A. Moldauer, Nucl. Phys., A344, 185(1980); see also Phys. Rev., C12, 744(1975).

27. E. Arthur and P. Young, Los Alamos Scientific Laboaratory Report, LA-8626-MS (1980).

Table I. Comparison of Observed and Reported Levels in ^{58}Ni

No.	E_x (MeV), Observed	E_x (MeV) (J^π), Ref. 17
1	1.458 ± 0.009	1.454 (2+)
2	2.462 ± 0.010	2.459 (4+)
3	2.791 ± 0.015	2.776 (2+)
4	2.927 ± 0.012	2.903 (1+) 2.943 (0+)
5	3.059 ± 0.025	3.038 (2+)

Table II. Spherical Optical-potential Parameters*

Real Potential[a]	
Strength	$V = 51.18 - 0.4 \times E(MeV)$, MeV
Radius[b]	$r_v = 1.220$, F
Diffuseness	$a_v = 0.548$, F
Imaginary Potential[c]	
Strength	$W = 9.98$, MeV
Radius	$r_w = 1.176$, F
Diffuseness	$a_w = 0.536$, F

*In addition, a spin-orbit potential of the Thomas form with a strength of 8 MeV and size parameters of the real potential was employed.

[a]Saxon form.

[b]All radii expressed in the form $R_i = r_i \cdot A^{\frac{1}{3}}$.

[c]Saxon-derivative form.